Journal of Power Sources 188 (2009) 332–337

Contents lists available at ScienceDirect

Journal of Power Sources

journal homepage: www.elsevier.com/locate/jpowsour

Radio frequency oxygen–plasma treatment of carbon nanotube electrodes for electrochemical capacitors

Chuen-Chang Lin*, Hsien-Chieh Huang

Department of Chemical & Materials Engineering, National Yunlin University of Science and Technology, 123 University Road Sec. 3, Douliu, Yunlin 64002, Taiwan

ARTICLE INFO

Article history:
Received 8 August 2008
Received in revised form
20 November 2008
Accepted 20 November 2008
Available online 3 December 2008

Keywords:
Carbon nanotubes
Plasma treatment
Functional groups
Annealing
Electrochemical capacitors

ABSTRACT

Carbon nanotubes were modified by RF (radio frequency) oxygen–plasma at different power levels and times, and subsequently annealed at different temperatures. At the 1000th cycle of potential cycling, maximum specific capacitance of 128 F g^{-1} was obtained in 0.1 M H_2SO_4 and with better plasma treatment conditions (power = 100 W and time = 30 min) and annealing temperature (350 °C). These show its high electrochemical stability and good specific capacitance at a higher sweep rate of 100 mV s^{-1}. In addition, the higher the power and time, the higher the carbonyl functional group (C═O), leading to higher specific capacitance.

1. Introduction

Electrochemical capacitors are charge-storage devices which possess higher power density/longer cycle life than batteries [1–2] and higher energy density than conventional capacitors [3]. Their applications include hybrid power sources, backup power sources, starting power for fuel cells, and burst-power generation in electronic devices [4–8]. Electrochemical capacitors are classified into two types, electric double layer capacitors (EDLC) and pseudo-capacitors according to the energy-storage mechanisms. The capacitance of an EDLC arises from the separation of charge at the interface between the electrode and the electrolyte. However, pseudo-capacitance arises from redox reactions of electroactive materials with several oxidation states [1,9–13].

Carbon nanotubes have nanometer size, hollow structure, low ratio of micropores, high accessible surface area, low resistance, and high stability. These properties make them potentially suitable for fabrication of electrodes in electrochemical capacitors [3,14].

The specific surface areas and pore size distributions of carbon materials influence the capacitance [15–17]. In addition, functional group distributions on the surface of carbon materials also affect the capacitor performance [17,18]. Furthermore, methods for the modification of the physical and chemical properties of carbon materials include acid treatment [3], plasma treatment [15–18], etc. The modification of activated carbon fiber cloth (ACFC) electrodes was performed by cold plasma in Ar–O_2 atmosphere and the effect of its cold plasma treatment on the capacitor performance has been discussed according to functional groups and pore size distributions of the ACFC surface [17]. Cascarini De Torre et al. [19] stated that graphitized carbon black was oxidized in a cool oxygen–plasma and this treatment changed graphitized carbon black surfaces from hydrophobic to hydrophilic. Li and Horita [20] mentioned that the carbon black surface was modified by low temperature oxygen–plasma, such that it changed from hydrophobic to hydrophilic, and functional groups containing oxygen increased in number. Ionescu et al. [21] noted that multi-wall carbon nanotubes applied to gas sensitive thick-film layers were functionalized by an inductively coupled RF (radio frequency) oxygen–plasma and their oxygen concentrations increased with increasing power levels or times of plasma treatment. In our previous study [22], a maximum capacitance of 38 F g^{-1} was obtained for activated carbon with better/superior plasma treatment conditions: power = 300 W, time = 3 min, and volume flow rates of oxygen = 45 sccm.

This plasma treatment can modify the surface properties of carbon materials without changing their bulk properties [17]. Single-walled carbon nanotubes were annealed in air at increasing temperatures in the range from 300 to 550 °C for 1 h and the specific capacitance was higher at an annealing temperature of 350 °C [23]. In addition, the increase in specific capacitance of modified carbon materials is attributed to an increase in the amount of surface functional groups [24–27]. Thus, in this research, cobalt was sputtered

* Corresponding author. Tel.: +886 5 534 2601x4619 fax: +886 5 531 2071.
E-mail address: linchuen@yuntech.edu.tw (C.-C. Lin).

0378-7753/$ – see front matter © 2008 Elsevier B.V. All rights reserved.
doi:10.1016/j.jpowsour.2008.11.100

on graphite foil on which carbon nanotubes were directly grown by chemical vapor deposition (CVD), then a RF oxygen–plasma was used to modify the surface properties of carbon nanotubes, such as functional groups at different power levels/times, next they were annealed at different temperatures, and finally maximum capacitance at better conditions was sought. Subsequently, the packing density/diameter of carbon nanotubes grown directly on graphite foil were examined by electron microscopy, the nanostructures of carbon nanotubes were examined through a transmission electron microscope (TEM), and functional groups of the carbon nanotube electrode were investigated by X-ray photoelectron spectroscopy (XPS).

2. Experimental methods

Because of its higher specific surface area, lower specific resistance, and a higher percentage of mesopore size distribution, a graphite foil (1×1 or $1 \times 2\,cm^2$) was used and abraded with SiC paper and then rinsed ultrasonically with de-ionized water for 10 min. It was then etched in 6 M aqueous HCl at room temperature for 30 min and subsequently rinsed ultrasonically with de-ionized water for 10 min. Next, it was degreased ultrasonically in acetone until any surface grease was completely eliminated. Finally, it was rinsed with pure de-ionized water, and then oven-dried in air (50 °C) to constant weight.

The cobalt (Co) catalyst particles were deposited on the pretreated graphite foil substrate by reactive RF magnetron sputtering from a 3-in. disk Co (purity: 99.9%, purchased from SCM, Inc.) target in a vacuum chamber with a background pressure of 7×10^{-6} Torr. The distance between the target and the substrate was 10 cm. The sputtering time, sputtering pressure, sputtering power, and the volume flow rate of argon were maintained at 4 h, 5 mTorr, 50 W, and 25 sccm, respectively. Then, the sputtered graphite foil was weighed. Next, carbon nanotubes were grown on the Co-coated graphite foil using thermal chemical vapor deposition (CVD) with a gas mixture of C_2H_2 (50 sccm) and Ar (100 sccm) for 30 min at 700 °C. Finally, the carbon nanotube electrode was weighed.

The carbon nanotube electrode was placed into the reaction chamber ($85\,cm^3$) of the apparatus for plasma treatment (frequency: 13.56 MHz and maximum power: 1000 W). Then, the chamber was degassed to 10^{-5} torr. Next, 30 sccm of oxygen gas was introduced to the chamber to maintain its pressure at 0.3 Torr. Next, the carbon nanotube electrode was modified by RF plasma at different power levels (50, 75, and 100 W) and times (3, 10, and 30 min), and then reweighed. Finally, the modified carbon nanotube electrode was annealed at different temperatures (200, 350, and 500 °C) in air for 1 h.

Electrochemical measurements for the prepared electrodes were performed using an electrochemical analyzer (CH Instruments CHI 608B, USA). The three-electrode cell consisted of Ag/AgCl as the reference electrode, Pt as the counter electrode and the prepared carbon nanotube electrodes as the working electrode. The electrolytes were degassed with purified nitrogen gas before voltammetric measurements and nitrogen was passed over the solution during all the measurements. The solution temperature was maintained at 25 °C by means of circulating water thermostat (HAAKE DC3 and K20, Germany). The cyclic voltammetry (CV) was undertaken with a 0.1 M aqueous electrolyte (H_2SO_4). A CV scan rate of 100 mV s^{-1} in the range 0–1 V was used in all measurements except where stated. Capacitance is normalized to 1 g of carbon nanotubes except where stated.

The packing density and diameter of carbon nanotubes grown directly on graphite foil substrate were conducted by field emission scanning electron microscope (FE-SEM: JEOL JSM-6700F, Japan). In addition, the nanostructures of carbon nanotubes with/without plasma treatment or with/without annealing were examined through (JEOL JEM-2010, Japan). Furthermore, functional groups of the carbon nanotube electrode with plasma treatment or with/without annealing were explored by XPS (Fison VG. ESCA210, England).

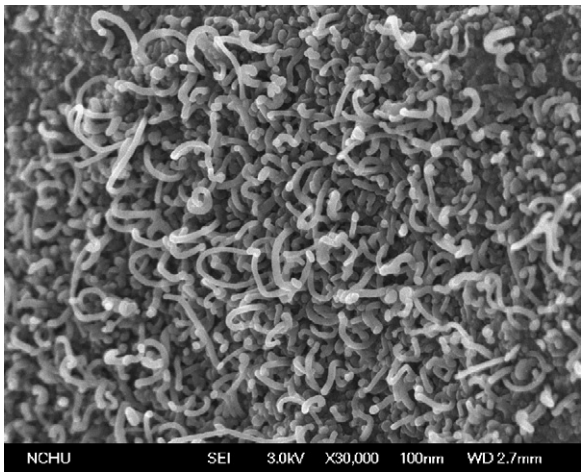

Fig. 1. FE-SEM micrograph of carbon nanotubes grown directly on graphite foil.

3. Results and discussion

Fig. 1 shows an FE-SEM micrograph of carbon nanotubes which were grown directly on the graphite foil. The packing density of the carbon nanotubes is about $5 \times 10^9\,cm^{-2}$ and the diameters as well as lengths of the carbon nanotubes are about 30–55 nm as well as 60–540 nm, respectively. In addition, the mesoporous network structure of carbon nanotube electrode favors the penetration of electrolytes due to the highly porous microstructure of carbon nanotube electrode shown in Fig. 1, then some active sites on inner or deeper layers are able to contribute to specific capacitance.

A CV curve at a potential scan rate of 100 mV s^{-1} in a 0.1 M H_2SO_4 solution for the carbon nanotube electrode without plasma treatment is shown in Fig. 2, which shows the nearly rectangular and symmetric current–potential characteristics of a capacitor with specific capacitance of 44 F g^{-1}. By contrast, a CV curve at a potential scan rate of 100 mV s^{-1} in a 0.1 M H_2SO_4 solution for the carbon nanotube electrode with better plasma treatment conditions (power = 100 W and time = 30 min) is shown in Fig. 3(a), which

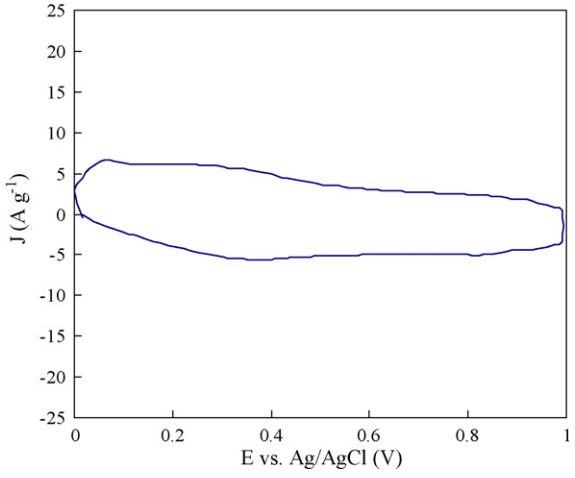

Fig. 2. A CV curve at a potential scan rate of 100 mV s^{-1} in a 0.1 M H_2SO_4 solution for the carbon nanotube electrode without plasma treatment.

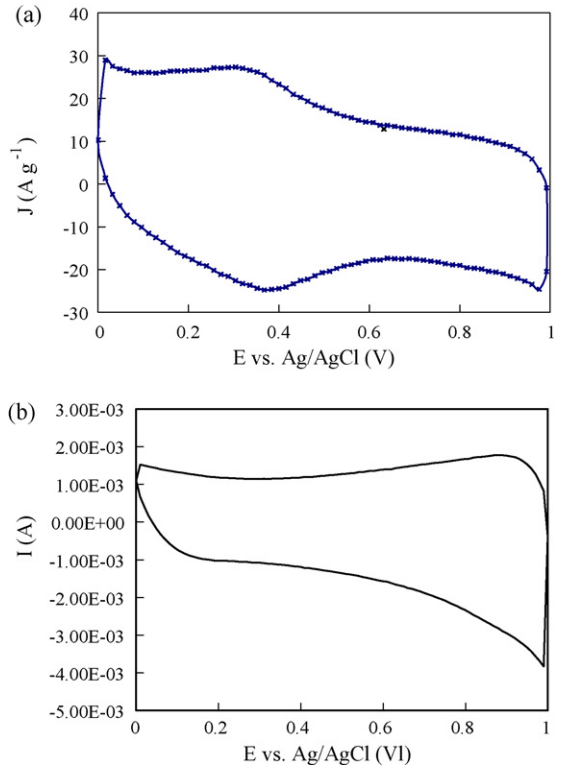

Fig. 3. A CV curve at a potential scan rate of 100 mV s^{-1} in a 0.1 M H_2SO_4 solution for the carbon nanotube electrode: (a) with better plasma treatment conditions (power = 100 W and time = 30 min) and (b) immersed in 15 wt.% HNO_3 aqueous solution.

shows a pair of redox peaks (an anodic peak and a cathodic peak) due to a Faradic process occurring in oxygen functional groups which were introduced on the surface of the carbon nanotubes after oxygen–plasma treatment. In addition, A CV curve for the raw carbon nanotube electrode immersed in 15 wt.% HNO_3 aqueous solution to remove the catalyst and also to increase surface oxygen groups with specific capacitance of 110 F g^{-1} is shown in Fig. 3(b), which agrees with the CV curve reported for other carbon nanotube electrode [16]. In addition, a CV curve for the raw carbon nanotube electrode treated with better plasma conditions with specific capacitance of 127 F g^{-1} is shown in Fig. 3(a), which agrees with the CV curves reported for other carbon nanotube electrodes [3,27]. Therefore, if there is some contribution to the specific capacitance of the carbon nanotube electrode from the catalyst and its oxides, it seems unimportant.

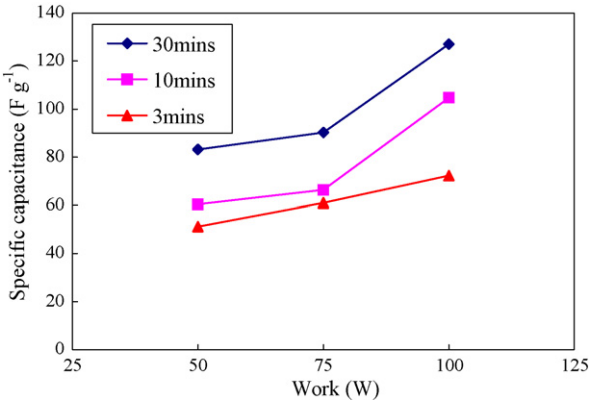

Fig. 4. Effects of power and time on the specific capacitance.

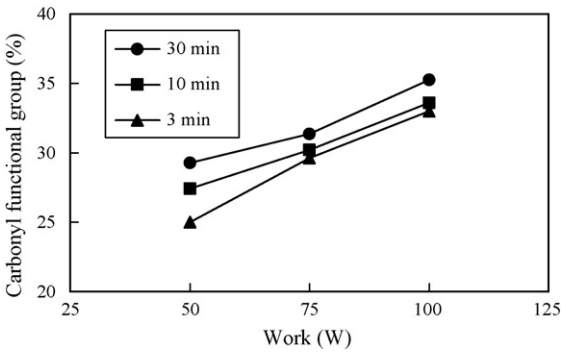

Fig. 5. Effects of power and time on the carbonyl functional group.

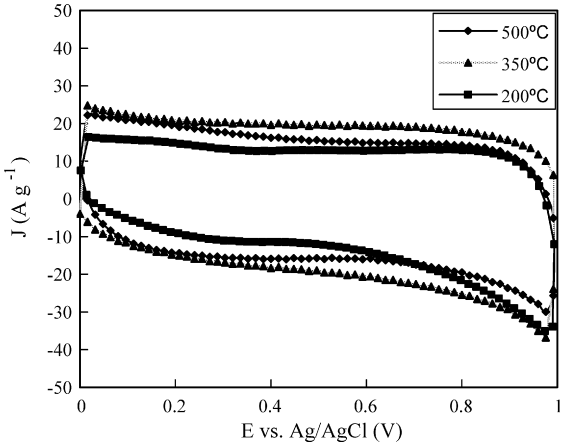

Fig. 6. CV curves at a potential scan rate of 100 mV s^{-1} in a 0.1 M H_2SO_4 solution for the carbon nanotube electrode with better plasma treatment conditions (power = 100 W and time = 30 min) and annealing temperature (200, 350, and 500 °C).

Fig. 4 shows effects of power and time on the specific capacitance, which reached a maximum (127 F g^{-1}) at the better plasma treatment conditions (power = 100 W and time = 30 min). Higher power leads to higher specific capacitance and longer time leads to higher specific capacitance. The reason behind this behavior may be that the higher the power and time, the greater the percentage of the carbonyl functional group (C=O) (see Fig. 5) at which fast faradic reactions take place and give rise to pseudo-capacitance (see Fig. 3), leading to higher specific capacitance (see Fig. 4). A similar result has been published in previous literature [24].

Table 1
XPS C 1s center binding energies (eV), functional groups, and areas (%) for carbon nanotubes modified by better plasma treatment conditions (power = 100 W and time = 30 min) with annealing and without annealing.

Annealing temperature (°C)	Peak	Functional group	Center Eb (eV)	Area (%)
200	1	Graphite	284.11	41.52
	2	Hydrocarbon	284.57	33.51
	3	Carbonyl	287.24	24.97
350	1	Graphite	284.22	39.43
	2	Hydrocarbon	284.96	20.87
	3	Carbonyl	287.56	39.70
500	1	Graphite	284.17	38.48
	2	Hydrocarbon	284.65	28.53
	3	Carbonyl	287.32	32.99
Without annealing	1	Graphite	284.13	38.65
	2	Hydrocarbon	284.68	26.07
	3	Carbonyl	287.23	35.25

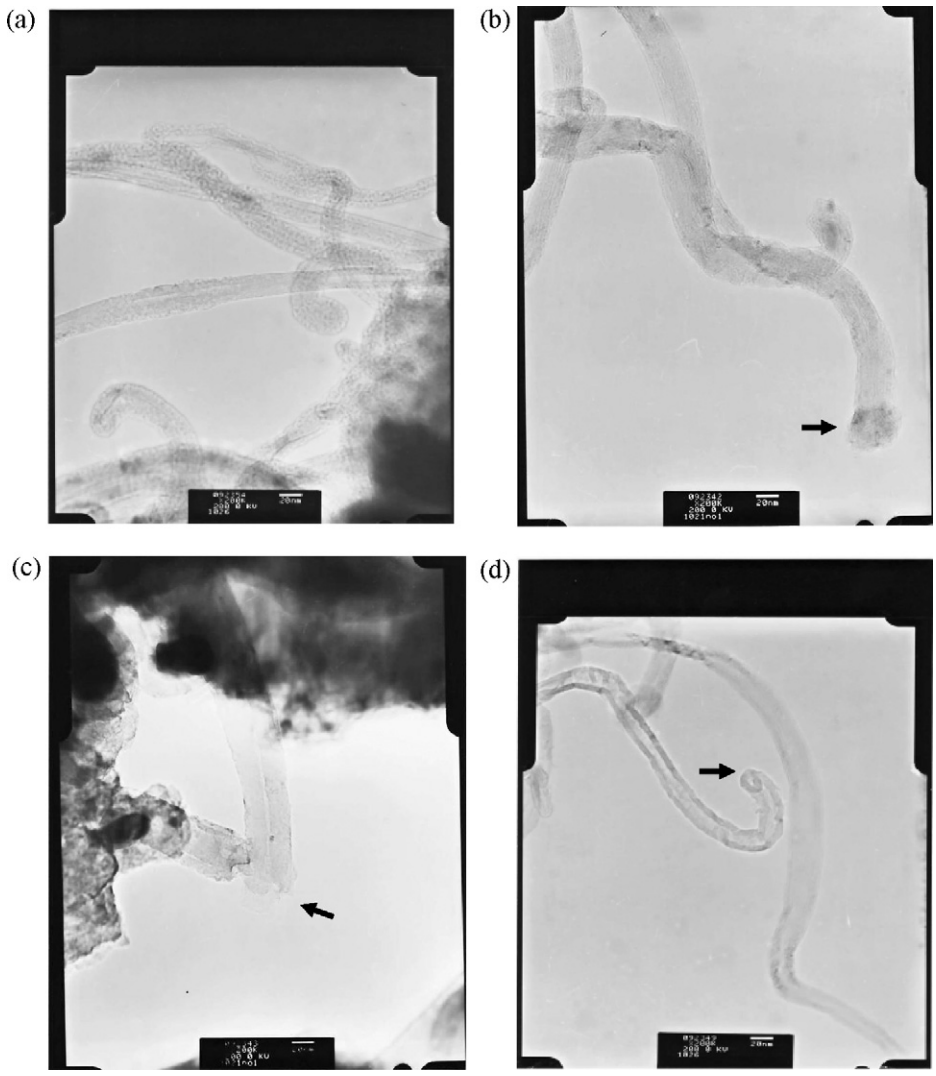

Fig. 7. TEM morphologies (the scale bar = 20 nm) of (a) the raw carbon nanotubes, (b) the raw carbon nanotubes modified by better plasma treatment conditions (power = 100 W and time = 30 min), (c) the raw carbon nanotubes modified by better plasma treatment conditions and with an annealing temperature of 350 °C, and (d) the raw carbon nanotubes modified by better plasma treatment conditions and with an annealing temperature of 500 °C.

CV curves at a potential scan rate of 100 mV s^{-1} in a 0.1 M H_2SO_4 solution for the carbon nanotube electrode with better plasma treatment conditions (power = 100 W and time = 30 min) and annealing temperature (200, 350, and 500 °C) are shown in Fig. 6, which shows the almost rectangular and symmetric current–potential except at potentials near the two limits of the potential window for an annealing temperature of 500 °C and the nearly rectangular and symmetric current–potential for an annealing temperature of 350 °C. In addition, the presence of surface oxygen groups has been ascribed to the formation of these groups either on the less organized and more reactive carbon materials or on the sidewall surfaces of nanotubes during oxygen–plasma treatment. However, removal of surface oxygen groups on the more reactive carbon materials and formation of new surface oxygen groups simultaneously occur during heat treatment in air. Furthermore, one pair of smaller redox peaks centered at around 0.3 V as well as another pair of larger redox peaks centered at around 0.45 V are attributable to the redox transitions of surface oxygen groups during the partial oxidation in air for carbon nanotubes [27]. Moreover, the oxygen (such as carbonyl groups in Table 1) responsible for CO evolution takes part in redox reactions, but the oxygen responsible for CO_2 evolution is of minor importance [26]. Therefore, the one pair of smaller redox peaks centered at around 0.3 V may be assigned to redox processes associated to CO_2-type surface oxygen groups. Then, a pair of redox peaks centered at around 0.3 V (see Fig. 3(a)) also might be assigned to redox processes associated to CO_2-type surface oxygen groups. Additionally, the intensity of CO_2

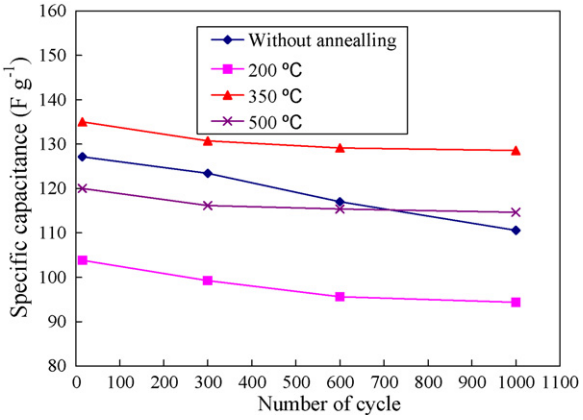

Fig. 8. Effects on specific capacitance of the carbon nanotube electrode modified by better plasma treatment conditions (power = 100 W and time = 30 min) without annealing and with annealing temperatures (200, 350 and 500 °C).

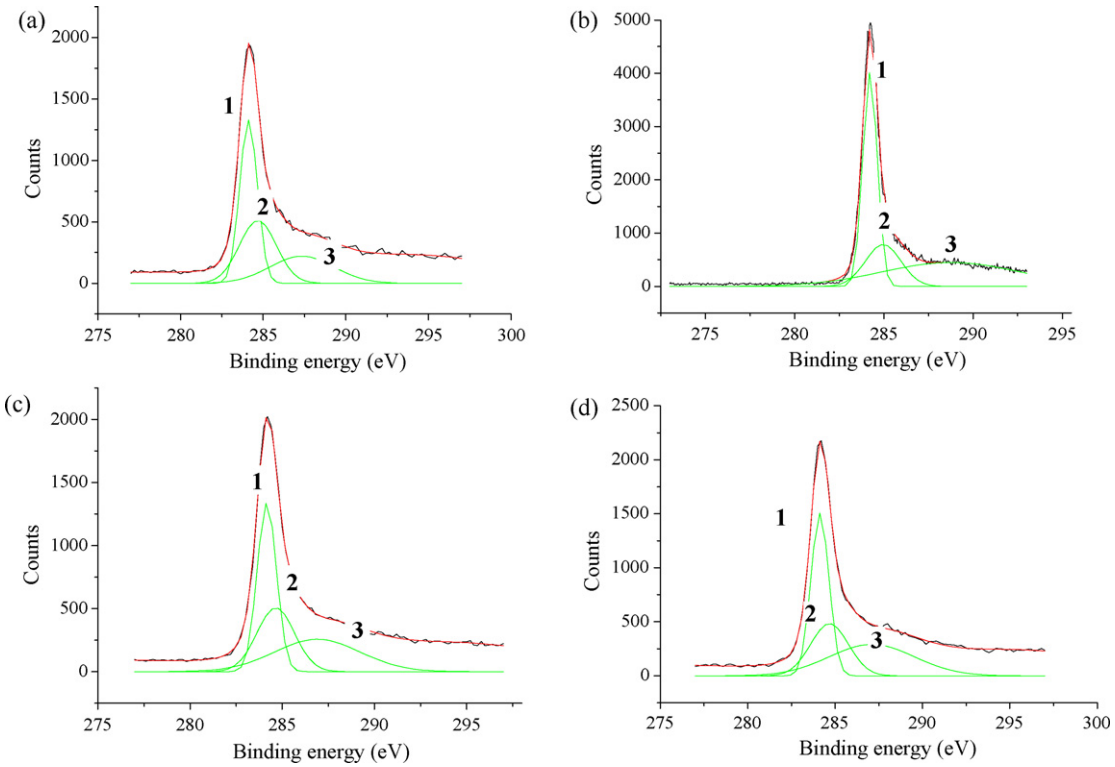

Fig. 9. XPS spectra in C 1s region for carbon nanotubes modified by better plasma treatment conditions (power = 100 W and time = 30 min) with annealing: (a) 200 °C, (b) 350 °C, and (c) 500 °C and (d) without annealing.

evolution between 190 and 500 °C is slightly reduced during the partial oxidation in air for carbon nanotubes [27]. So the carbon nanotube electrodes with better plasma treatment conditions and heat treatment (200, 350, and 500 °C) in air do not exhibit redox peaks in the CV curve (see Fig. 6). A similar CV curve reported for other carbon nanotube electrode annealed in air at 350 °C has been published in previous literature [23].

By the oxygen–plasma process (power = 100 W and time = 30 min), the weight loss is about 14 wt.%, then the closed ends of nanotubes are uncapped (See the arrow in Fig. 7(b)) and certain defects seem to be formed on sidewall surface of nanotubes compared to the raw carbon nanotubes (see Fig. 7(a) and (b)). Opening the closed ends and rough "convex-concave" walls of nanotubes enlarge the specific surface area, which leads to simultaneously increasing formation of new surface oxygen groups and the specific capacitance of the carbon nanotube electrode. In addition, the raw carbon nanotubes modified by better plasma treatment conditions (power = 100 W and time = 30 min) and with annealing temperatures of 350 and 500 °C do not significantly differ from the raw carbon nanotubes modified by better plasma treatment conditions. However, the raw carbon nanotubes modified by better plasma treatment conditions and with annealing temperatures of 350 and 500 °C show more integral sidewall surfaces and clear openings (see the arrows in Fig. 7(b)–(d)) of nanotubes compared to the raw carbon nanotubes modified by better plasma treatment conditions, and the higher the annealing temperature, the higher the percentage of the weight loss (such as 350 °C: only 18 wt.% and 500 °C: only 23 wt.% due to 14 wt.% of the weight loss through oxygen–plasma treatment before annealing), the more integral sidewall surface and observable opening of nanotubes (see Fig. 7(b)–(d)).

Fig. 8 shows effects on specific capacitance of the carbon nanotube electrode modified by better plasma treatment conditions (power = 100 W and time = 30 min) without annealing and with annealing temperatures (200, 350 and 500 °C). At the 1000th cycle of potential cycling, the electrode annealed at a temperature of 350 °C possessed the highest specific capacitance value of 128 F g^{-1}. In addition, at the 15th cycle of potential cycling, the specific capacitance of the carbon nanotube electrode with an annealing temperature of 350 °C was maximum due to its highest carbonyl functional groups (C=O) (see Table 1 and Fig. 9). A similar annealing result has been published in previous literature [23]. Furthermore, the specific capacitance of the carbon nanotube electrode without annealing decreased quickly with increasing number of charge–discharge cycles, but the specific capacitance of the electrode with annealing gradually decreased with increasing number of charge–discharge cycles and the higher the annealing temperature, the slower the decreasing rate of the specific capacitance. The reason behind this behavior may be that the less organized and more reactive carbon material is removed after heat treatment in air, then the crystalline CNT content is higher and also the reversibility of the CV curves (see Figs. 3 and 6) as well as electrochemical stability in the specific capacitance values with cycling (see Fig. 8) are higher due to more easily losing the less organized carbon material through gradual partial dissolution or detachment during the charge–discharge cycles. In addition, the higher the annealing temperature, the more the amount of the less organized and more reactive carbon material removed (such as 350 °C: 18 wt.% and 500 °C: 23 wt.%), then the higher the crystalline CNT content, the better the reversibility of the CV curve (see Fig. 6) and the slower the decreasing rate of the specific capacitance (see Fig. 8).

4. Conclusion

RF oxygen–plasma and annealing treatments were employed to modify carbon nanotubes and obtain maximum capacitance at better conditions. The specific capacitance increased with increasing plasma power levels and times. In addition, the closed ends of nanotubes are opened through oxygen–plasma treatment. Furthermore, the maximum specific capacitance of the carbon nanotube

electrode was obtained with an annealing temperature of 350 °C. Moreover, the specific capacitance of the carbon nanotube electrode without annealing decreased quickly with increasing number of charge–discharge cycles. However, the specific capacitance of the electrode with annealing gradually decreased with increasing number of charge–discharge cycles due to the higher crystalline CNT content after annealing and the higher the annealing temperature, the higher the crystalline CNT content, the slower the decreasing rate of the specific capacitance.

References

[1] B.E. Conway, Electrochemical Supercapacitors–Scientific Fundamentals and Technological Applications, Kluwer Academic/Plenum Publishers, New York, 1999.
[2] R. Kotz, M. Carlen, Electrochimica Acta 45 (2000) 2483–2498.
[3] J.H. Chen, W.Z. Li, D.Z. Wang, S.X. Yang, J.G. Wen, Z.F. Ren, Carbon 40 (2002) 1193–1197.
[4] Y.S. Chen, C.C. Hu, Electrochemical and Solid-State Letters 6 (10) (2003) A210–A213.
[5] Y.U. Jeong, A. Manthiram, Journal of The Electrochemical Society 149 (11) (2002) A1419–A1422.
[6] C.C. Hu, C.C. Wang, Journal of The Electrochemical Society 150 (8) (2003) A1079–A1084.
[7] H.P. Park, O.O. Park, K.H. Shin, C.S. Jin, J.H. Kim, Electrochemical and Solid-State Letter 5 (2) (2002) H7–H10.
[8] R.N. Reddy, R.G. Reddy, Journal of Power Sources 124 (2003) 330–337.
[9] A. Burke, Journal of Power Sources 91 (2000) 37–50.
[10] J.K. Chang, W.T. Tsai, Electrochemistry Communications 6 (2004) 666–671.
[11] M.S. Hong, S.H. Lee, S.W. Kim, Electrochemical and Solid-State Letters 5 (2002) A227–A230.
[12] J.H. Park, J.M. Ko, O.O. Park, Journal of The Electrochemical Society 150 (7) (2003) A864–A867.
[13] J.R. Zhang, B. Chen, W.K. Li, J.J. Zhu, L.P. Jiang, International Journal of Modern Physics B 16 (2002) 4479–4483.
[14] C. Li, D. Wang, T. Liang, X. Wang, Powder Technology 142 (2004) 175–179.
[15] H. Shi, Electrochimica Acta 41 (1996) 1633–1639.
[16] E. Frackowiak, F. Beguin, Carbon 39 (2001) 937–950.
[17] M. Ishikawa, A. Sakamoto, M. Morita, Y. Matsuda, K. Ishida, Journal of Power Sources 60 (1996) 233–238.
[18] C.T. Hsieh, H. Teng, Carbon 40 (2002) 667–674.
[19] L.E. Cascarini De Torre, E.J. Bottani, A. Martinez-Alonso, A. Cuesta, A.B. Garcia, J.M.D. Tascon, Carbon 36 (1998) 277–282.
[20] X. Li, K. Horita, Carbon 38 (2000) 133–138.
[21] R. Ionescu, E.H. Espinosa, E. Sotter, E. Llobet, Sensors and Actuators B 113 (2006) 36–46.
[22] C.C. Lin, C.C. Yen, Journal of Applied Electrochemistry 37 (7) (2007) 813–817.
[23] F. Pico, J.M. Rojo, M.L. Sanjuan, A. Anson, A.M. Benito, M.A. Callejas, Journal of The Electrochemical Society 151 (2004) A831–A837.
[24] M.J. Bleda-Martínez, J.A. Maciá-Agulló, D. Lozano-Castelló, E. Morallón, D. Cazorla-Amorós, A. Linares-Solano, Carbon 43 (2005) 2677–2684.
[25] M.J. Bleda-Martínez, D. Lozano-Castelló, E. Morallón, D. Cazorla-Amorós, A. Linares-Solano, Carbon 44 (2006) 2642–2651.
[26] V. Ruiz, C. Blanco, E. Raymundo-Piñero, V. Khomenko, F. Béguin, R. Santamaría, Electrochimica Acta 52 (2007) 4969–4973.
[27] C.C. Hu, J.H. Su, T.C. Wen, Journal of Physics and Chemistry of Solids 68 (2007) 2353–2362.